



## Corrosion and Microhardness Behavior Improvement of 316L Stainless Steel via Fiber Laser Surface Treatment

Mustafa Majid <sup>1\*</sup>, Enas A. Khalid <sup>2</sup> and Hayder Zghair <sup>3</sup>

<sup>1,2</sup> Department of Automated Manufacturing Engineering, Al-Khwarizmi collage of Engineering, University of Baghdad, Iraq

<sup>3</sup> Department of Engineering, College of Science and Engineering, Southern Arkansas University (USA)

\*Corresponding Author's E-mail: [mostafa.ali2240m@kecbu.uobaghdad.edu.iq](mailto:mostafa.ali2240m@kecbu.uobaghdad.edu.iq)

(Received 19 June 2023; Revised 4 November 2023; Accepted 25 December 2023; Published 1 December 2024)

<https://doi.org/10.22153/kej.2024.12.002>

### Abstract

This study investigated how fibre laser surface treatment affects stainless steel 316L's microhardness and corrosion resistance. The laser parameters utilized in this investigation were four different readings of laser power applied at a constant frequency and scanning speed to stainless steel 316L specimens. A digital micro-Vickers hardness tester was used to measure the microhardness of the samples before and after laser treatment. The TAFEL cyclic potentiodynamic polarization technique was employed to study corrosion behaviour. The microstructure of the base metal and the effect of laser power were investigated using optical microscopy. The phases before and after laser treatment were identified through X-ray diffraction, and the cross section of the heat-affected zones and the molten pool's depth were examined using a scanning electron microscope. Results revealed that laser treatment affected microstructural transitional phase alterations. Compared with the average microhardness of the base metal, the microhardness of the laser-treated specimens improved to 78.23% as the laser power increased. The increase in microhardness considerably enhanced corrosion resistance to 36.13% relative to that of the base metal.

**Keywords:** Corrosion; Fiber Laser; Microhardness; SS316L; Surface Treatment

### 1. Introduction

Lasers can be utilized as highly adaptable, mouldable thermal sources. Lasers can alter the surface properties of specific materials. The high power density and short contact times of lasers produce high heating rates in a thin surface layer. After surface treatment, self-quenching causes fast cooling, which in turn introduces microstructural alterations, such as grain refinement or phase transitions to metastable phases. Additional microstructural changes, such as the dissolution or modification of precipitates or residual stresses, alter the surface and subsurface properties of the material. Laser surface treatments are considered a well-established method to improve corrosion resistance and surface hardness [1].

Lasers have many exceptional properties, such as non-contact processing, improved product quality, low cost, high production, decreased finishing operations and processing, high material use and a small heat-affected zone. The need for laser material processing is increasing because of these properties [2]. The usage of lasers for material processing may be classified into two groups: (a) uses that require minimal energy or power and do not appreciably affect phases and (b) uses that require a considerable amount of energy to accomplish. The first group includes processes for annealing and etching semiconductors, curing polymers and labelling integrated circuit substrates. The second group comprises cutting, welding, melting and heat treatment [3]. Engineering material failure can be categorized into numerous categories: corrosion, oxidation, fatigue and wear/abrasion. Material

This is an open access article under the [CC BY](https://creativecommons.org/licenses/by/4.0/) license:



failure may start at the surface because of two main factors: vulnerability of free surfaces to environmental deterioration and high intense external load at the surface. To eliminate failure that starts at the surface, engineers can alter the surface microstructure and composition of the near-surface region of a component without changing the bulk [4,5]. The most popular conventional surface engineering methods are galvanizing, diffusion coating, carburizing, nitriding and flame/induction hardening. However, these methods have several drawbacks, such as low precision, limited flexibility range and high time, energy and material consumption.

Ti alloys, Co alloys and stainless steels are frequently used for biomedical implant purposes. Metals and their alloys are essential to structural biomaterials used in reconstructive surgery, especially orthopedics. Given that the surfaces of these metals and their alloys are prone to corrosion, laser technology is employed to alter their mechanical characteristics (e.g. hardness). The majority of laser surface modifications has been applied to ferritic (430), martensitic (420) and austenitic (304) stainless steels to reinforce their resistance to pitting corrosion. The most common implant material is 316L austenitic stainless steel because it is inexpensive [6]. Austenitic stainless steel is one of the most frequently utilized alloys in maritime, biomedical and aerospace industries because of its superior flexibility and corrosion resistance [7]. Stainless steel 316L (SS316L) is excellent for corrosion resistance applications because it can form a coherent, adhesive, oxide-thin layer of chromium ( $\text{Cr}_2\text{O}_3$ , a corrosion barrier). However, this layer of oxide chromium created on the surface of the implant metal is unstable because the layer tends to localize corrosion in long-term implant applications. Moreover, the human body is a complex and challenging electrolytic environment for biomaterial applications [8,9]. The corrosion protection provided by laser treatment is attributed mainly to the grain refinement of the top surface layer [10]. Grain refinement can improve strength, such that a reduction does not create microporosity [11]. Numerous investigations have been performed to enhance the surface qualities, such as corrosion resistance, wear and hardness, of metals and alloys because of these materials' importance in daily life.

For AISI SS316L, the processes of low-energy, high-current pulsed electron beam (LEHCPEB) corrosion and wear improvements were studied by Zou et al., who found that AISI SS 316L confirms the high potential of the LEHCPEB technique for improving the aforementioned properties, particularly when the number of pulses is

sufficiently high [12]. Muna investigated the effects of ND:YAG laser treatment on the surface modification and corrosion behaviour of the most popular implant biomaterial (SS316L) in an artificial saliva solution at a temperature of 37 °C. The results showed that a decrease in the pulse repetition rate or frequency from 1 Hz to 6 Hz at 1,064 nm results in surface modification, grain refinement and a slight improvement in hardness. Corrosion tests revealed that the samples treated with 1 Hz at 532 and 1,064 nm had higher corrosion resistance than the untreated base alloy and other treated samples [13]. Abbas et al. examined how pulsed laser surface melting affects AISI 304 stainless steel's corrosion and wear properties. The results demonstrated that LSM enhances the hardness and wear resistance of treated samples. The corrosion test also revealed that treated samples have stronger resistance to pitting corrosion than untreated ones [14]. Singh et al. studied the effects of laser surface processing on the surface microstructure and corrosion behaviour of SS316L and Ti-6Al-4V. They found that metal ions are generated during the corrosion process (laser power of 500–1,500 W) in an ambient environment. In the re-solidified area of SS316L, columnar dendrites and tiny grains create a homogeneous surface microstructure. The researchers also discovered that grain size gradually increases from the substrate towards the treated surface. Compared with the corrosion characteristics of untreated counterparts, the corrosion characteristics of Ti-6Al-4V improve, whereas those of SS316L worsen after laser processing. SS316L's corrosion resistance is affected by variations in laser power, but that of Ti-6Al-4V is not substantially affected [15]. Tangkwampian et al. studied the influence of fibre laser surface modification on the corrosion behaviour of SS316L and found that laser treatment increases the pitting potential by 40%. The results also showed a shift in corrosion potential to a more favourable one. The corrosion improvement results led to the conclusion that the corrosion protective layer on the newly laser-treated surface can reduce the material's pitting tendency [16]. Ganesh Dongre revealed the effects of different laser parameters on the microhardness of SS316L after laser hardening. They obtained a 25% increase in hardness after laser hardening and a hardened depth of up to 400 microns [17]. Bakhtiari et al. used a high-power ND:YAG pulsed laser at a maximum power of 3.5 kW to study the hardness of AISI4130 steel. Some of the results showed that the coefficient of friction decreases from 0.77 in the base metal to 0.39 in the hardened samples [18].

Previous researchers have investigated and used several laser methods, including laser surface hardening and melting, with a continuous wave and pulsed mode under different laser parameters, such as power density, beam power, travel speed and pulse duration.

This study investigates fibre laser surface treatment and the effects of laser power on the microhardness, corrosion resistance and microstructure of SS316L by using a high frequency (KHz), high scanning speed, and very small spot size ( $\mu\text{m}$ ).

## 2. Materials and Methods

**Table 1.**

**SS316L's chemical composition.**

	Element	C	Si	Mn	P	S	N	Cr	Mo	Ni	Fe
<b>Actual test</b>	Value %	0.027	0.3	1.38	0.03	0.004	0.09	17.1	2.03	11.5	Bal.
<b>standard</b>	Value %	$\leq$	0.75	2	0.045	0.03	0.1	16.5–18.5	2–2.5	10–14	Bal.
		0.03									

**Table 2.**

**Mechanical properties of SS316L [19].**

Density- $\text{kg}/\text{m}^3$	8,000
Micro hardness-HV	206.3
Modulus of elasticity-GPa	193
Thermal conductivity at 20 °C W/m K	15
Specific heat-0 °C –100° C ( J/kg.K)	500

## 2.2 Methods

The first step in sample preparation was cutting the samples into cylindrical shapes with dimensions of (4×9, 5×10, 20×10 and 8×20 mm) in height and diameter, as shown in Figure (1). The samples were ground using silicon carbide (Sic) paper with different grids (220, 400 and 800) for corrosion, microhardness, scanning electron microscopy (SEM) and X-ray diffraction (XRD) tests. The samples were ground using Sic paper with grids of 220, 400, 600, 800, 1,200 and 2,000 for the microstructure test, and the samples were micro-polished with a diamond suspension of 0.1  $\mu\text{m}$  particle size to achieve a good finish for vivid findings. Next, alcohol was employed to wash the samples and remove oils from the surface to obtain precise details of the microstructures under a microscope. The cross-section surfaces were etched for 60 s by using Marable's reagent etchant solution [20]. Marable's etchant contains 50 mL of HCL, 50 mL of  $\text{CuSO}_4$  and 10 mL of distiller water. The etched samples were dried in an oven after being rinsed with distilled water and alcohol. The microstructure of the base metal and the effect of laser spot size with various laser power were

## 2.1 Materials

The material used in this study was wrought SS316L. Austenitic SS316L was utilized in this study because of its vast application in the biomedical field, and it is used in orthopedics and dental implants. This steel is a rolled sheet with 30 mm thickness. Table (1) shows SS316L's chemical composition, and Table (2) presents its mechanical properties.

investigated through optical microscopy. The cross-sectional area of the heat-affected zones and the molten pool's depth were examined SEM. The phases before and after laser treatment were identified via XRD. A digital micro-Vickers hardness tester was used to measure the microhardness of the samples in HV before and after laser treatment, and a microhardness test was conducted at a load 1 kg for 15 s. The TAFEL cyclic potentiodynamic polarization technique and the WINKING M Lab 200 potentiostat from Bank-Elektronik software were employed to examine the corrosion behaviour. The samples were immersed in seawater solution for an electrochemical corrosion test for 15 min.

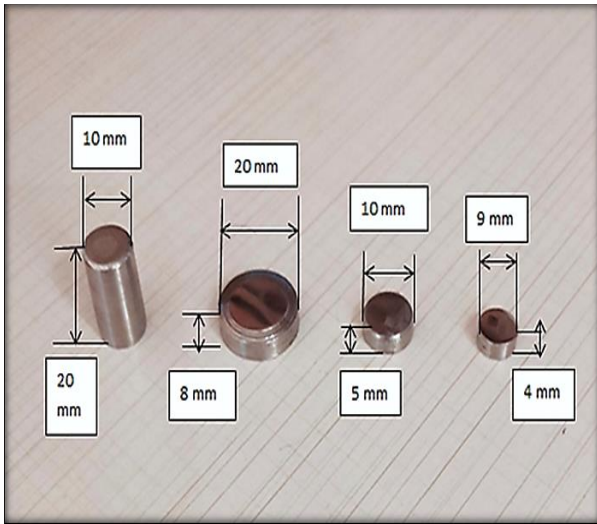


Fig. 1. Types of samples used in this study.

### 2.2.1 Laser System Specifications

A laser beam was used as a heat source to enhance the surface metal’s characteristics through phase changes. The specifications of the laser device used in the surface treatment are listed in Table (3), and the laser parameters are given in Table (4). The device is shown in Figure (2).

The EzCad2 software program was used to determine the laser power, laser scanning speed and laser frequency for this study. In this software, the laser path can be determined by Hatch. The Zigzag path was used in this study because of its popularity and efficiency.

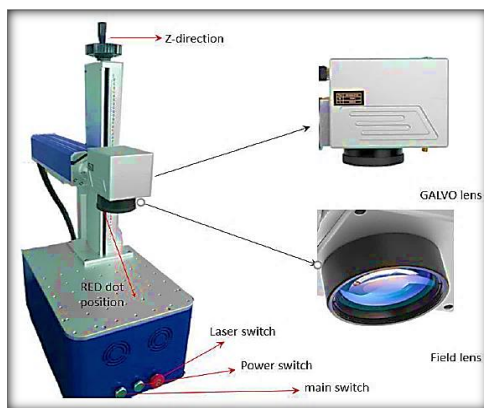
This work was performed in AL-Nahrain University Laser and Optoelectronics Engineering Department.

Table 3. Specification of the laser machine used in this work.

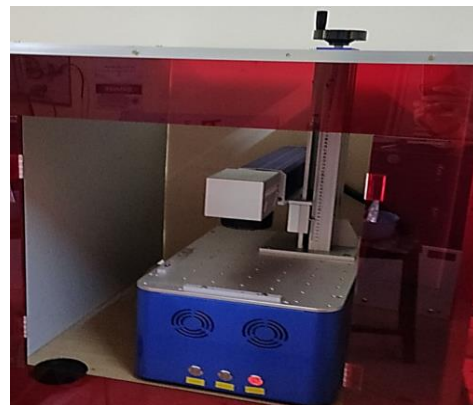
Specification	Description	Units
Brand name	Wuxi Raycus Fiber Laser Technologies Co., Ltd.	-
Type	Fiber optics laser	-
Origin	China	-
Power	0–31	W
Scanning speed	0–6000	mm/s
Frequency	30–60	KHz
Applications	Surface processing, marking, engraving	-

Table 4. Variable fibre laser power with other parameters being constant.

No.	Parameters	Values	Units
1	Power	3, 5, 7.5, 10	W
2	Scanning speed	3,000	mm/s
3	Frequency	30	KHz
4	Wavelength	1,064	nm
5	Spot size	70	µm
6	Pulse duration	127	ns
7	Working distance	20	cm
8	Medium	air	-



(a)



(b)

Fig. 2. Laser device system: (a) fibre laser device and (b) components of the fibre laser device.

### 2.3 Microhardness test

This microhardness test determined the material's hardness or resistance to the penetration of the indenter. The Vickers hardness test method employed a digital device (Vickers hardness tester TH714). The main parts of this device are the microscope, indenter, screw and testing table, as shown in Figure (3). The diamond indenter was indented in the test material as a pyramid with a square base and a top angle of  $136^\circ$  between opposite faces subjected to a load of 9.8 N. The full load of 9.8 N was normally applied for 15 s. Three readings were obtained, and the averaged values represent the microhardness of all the samples (as received and treated).

This task was performed in University of Baghdad, Al-Khwarizmi College of Engineering, Automated Manufacturing Engineering Department, Iraq. Hardness was measured using Vickers' law as follows [21]:

$$HV = 1.854 \frac{P}{d^2}, \quad \dots (1)$$

where HV is Vickers hardness ( $kg\ f/mm^2$ ), P is the load applied (kg f) and D is the indentation diameter (mm).



Fig. 3. Microhardness test device.

### 2.4 Corrosion Test

Cylindrical samples measuring 20 mm in diameter and 8 mm in height, as shown in Figure (1), were immersed in seawater (3.5 wt.% NaCl solution) at 25 °C for an electrochemical corrosion

test. Cycle polarization experiments were conducted using the WINKING M Lab 200 potentiostat from Bank-Elektronik and a standard electrochemical cell, as indicated in Figure (4). Fifteen minutes of electrochemical measurements were performed with the potentiostat at a scan rate of 3 mV/sec. The key results were expressed in terms of corrosion potential ( $E_{corr}$ ) and corrosion current density ( $I_{corr}$ ). The Tafel slopes were also measured in this study [22]. This examination was done in the Ministry of Science and Technology's Inspection of Materials Laboratory.

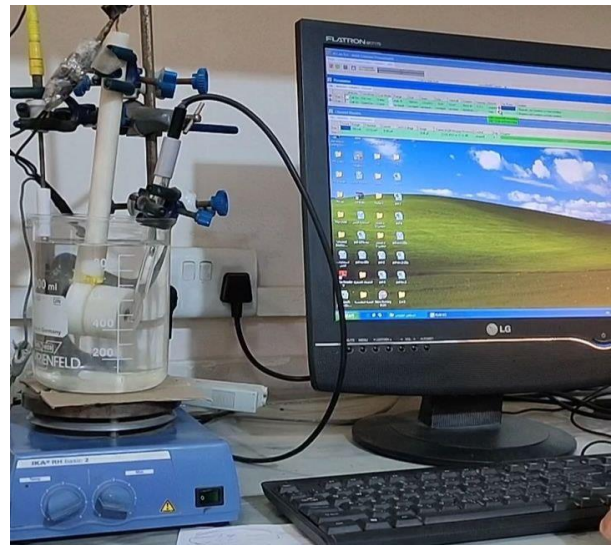


Fig. 4. Electrochemical corrosion cell test.

## 3. Results and Discussions

### 3.1 Effect of Laser Power on Microhardness

Table (5) shows the measured microhardness of the samples treated at different laser power with a constant speed and frequency on the SS316L metal surface.

The highest value of microhardness (367.7 HV) was found in Sample (A3), and the lowest value of microhardness (183.8 HV) was in the Sample (A4). The base metal's value was 206.3 HV, as shown in Table (5) and Figure (3).

**Table 5.**  
Effect of laser power on the microhardness of SS316L.

Sample	Power (W)	Speed (mm/s)	Frequency (KHz)	Microhardness readings			Average microhardness (HV)	% improvement
				1	2	3		
Base Metal SS316L	-	-	-	213.0	205.2	199.6	206.3	-
A1	3	3,000	30	211.3	197.8	196.1	201.7	- 2.22 %
A2	5	3,000	30	228.9	211.0	205.0	214.9	+ 4.16 %
A3	7.5	3,000	30	373.1	367.9	362.1	367.7	+ 78.23 %
A4	10	3,000	30	197.6	184.1	169.8	183.8	- 10.9 %

The increase in microhardness in most of the treated samples was due to grain refinement of the metal surface [23,24]. This study revealed that increasing the laser power from 3 W to 7.5 W increased the microhardness of the surface metal, but increasing the laser power from 7.5 W to 10 W decreased the microhardness of the metal surface. This decrease was due to the relationship between laser power and the melted surface [25]. Figure (3) shows the effect of laser power on the microhardness of the surface metal.

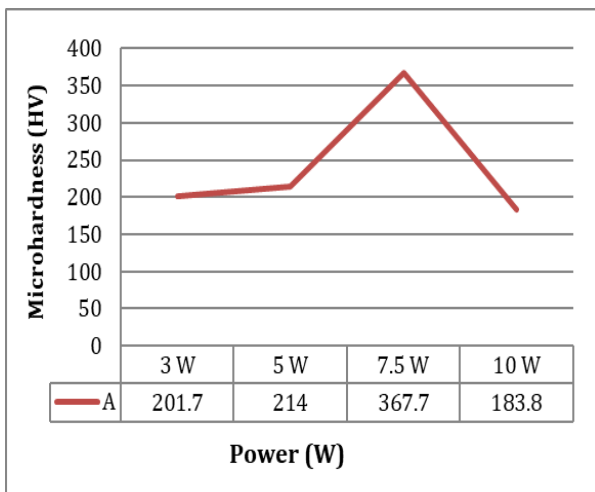


**Fig. 3.** Effect laser power on microhardness.

### 3.2 Effect of Laser Power on Corrosion Resistance

Table (6) shows the influence of lasers on the electrochemical corrosion test done in NaCl solution (3.5 wt.%). The sample chosen for the corrosion test depended on the highest readings of the microhardness test, and a comparison was made with the base metal. The cyclic polarization curve for Sample A shows the result of the untreated sample, and that for Sample B shows the result of the laser-treated sample. Figure (4a) presents the cyclic polarization curve for the base metal (SS316L). On the basis of the corrosion test in NaCl solution (3.5 wt.%), pitting corrosion (loop cycle) was observed. This figure contains Tafel and cyclic polarization curves. The Tafel equation was utilized to determine the corrosion rate (in material per year). The results showed that pitting corrosion increased when the corrosion current ( $I_{corr}$ ) increased, as indicated in Table (6). Meanwhile, corrosion behaviour (pitting corrosion) decreased with the loop cycle compared with that in Sample (A), as indicated in Figure (4b).

**Table 6.**  
Corrosion results for the base metal and laser-treated sample.

Samples	Power (W)	Speed (mm/s)	Frequency (KHz)	I corr. (nA/cm <sup>2</sup> )	E corr. (mV)	Corrosion rate (material per year = 0.43)	% Improvement
Base metal							
(A)	-	-	-	283.51	-331.5	121.9	-
(B)	7.5	3000	30	18.71	-211.7	8.0	+ 36.13 %

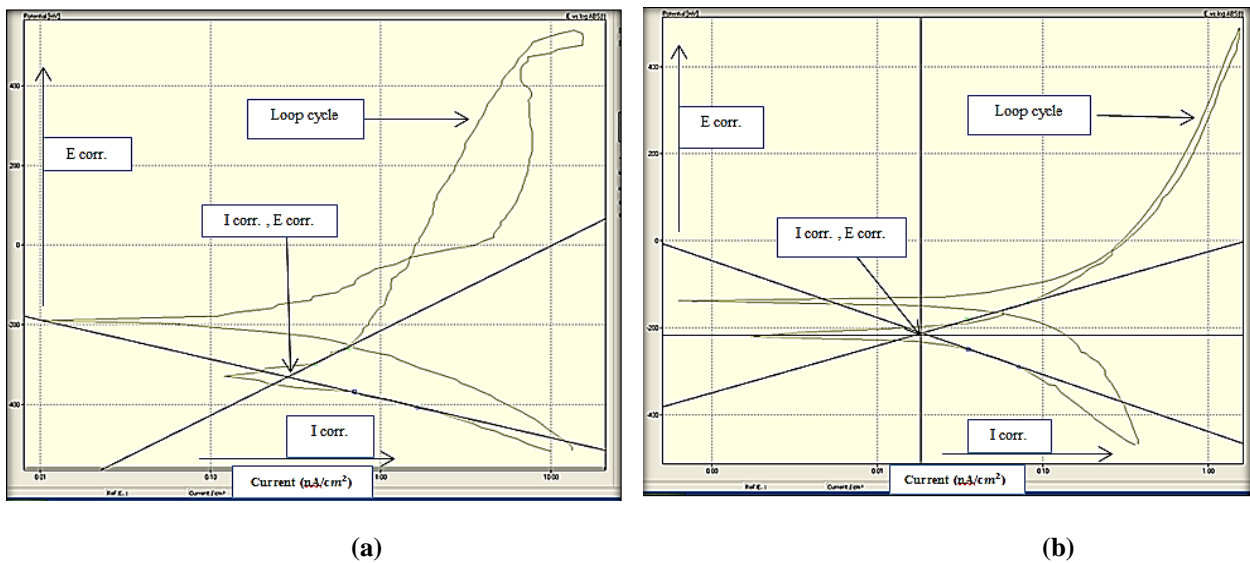


**Fig. 4.** Corrosion results of (a) base metal Sample A (before laser treatment) and (b) Sample B (after laser treatment).

The results of the corrosion tests showed that the corrosion resistance of the laser-treated sample was better than that of the untreated sample. This improvement in corrosion resistance confirmed that a layer of chromium oxide was formed as a protective layer on the surface; it slowed down corrosion and improved the resistance to pitting corrosion [14,15,16].

### 3.3 Effect of Laser Power on the Microstructure of SS316L

The laser parameters affected the metal surface and surface morphology, leading to an increase in the intensity of the austenite phase ( $\gamma$ -Fe) due to grain refinement [23,24] and showing the presence of the alpha ferrite phase ( $\alpha$ -Fe), as presented in Table (7).

**Table 7.**  
XRD data.

Sample	Power (W)	Speed (mm/s)	Frequency (KHz)	Average microhardness (HV)	XRD phases
Base metal SS316L	-	-	-	206.3	$\gamma$ -Fe
A3	7.5	3000	30	367.7	$\gamma$ -Fe + $\alpha$ -Fe

The microstructure of the base metal SS316L before and after laser treatment is shown in Figure (5). It explains the grain structure and phases of SS316L, which consists of an austenite phase with a regular distribution of grain boundaries with twin

boundaries. XRD explained the phase transformation, as shown in Figure (6). The sample chosen for the XRD test depended on the highest readings of the microhardness test, and a comparison was made with the base metal.

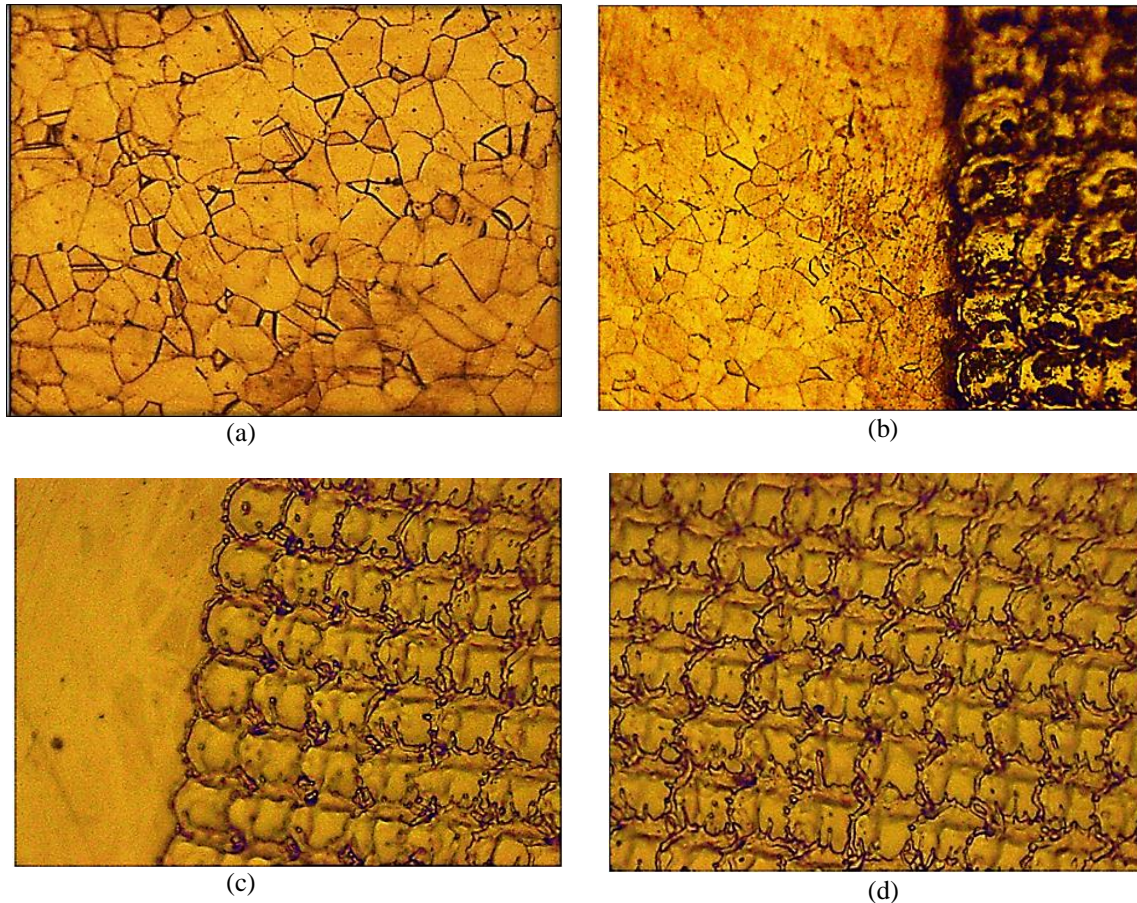


Fig. 5. Microstructure of SS316L at 400×. (a) Base metal after etching using Marable's etchant. (b) Laser-treated sample at laser power of 7.5 W, scanning speed of 3,000 mm/s and frequency of 30 KHz after etching. (c and d) Laser-treated sample at laser power of 7.5 W, scanning speed of 3,000 mm/s and frequency 30 KHz before etching.

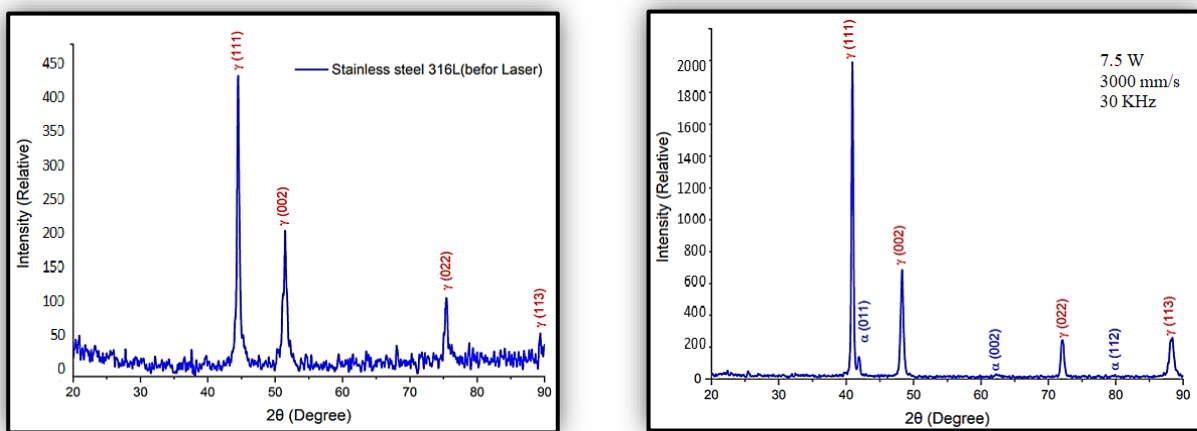


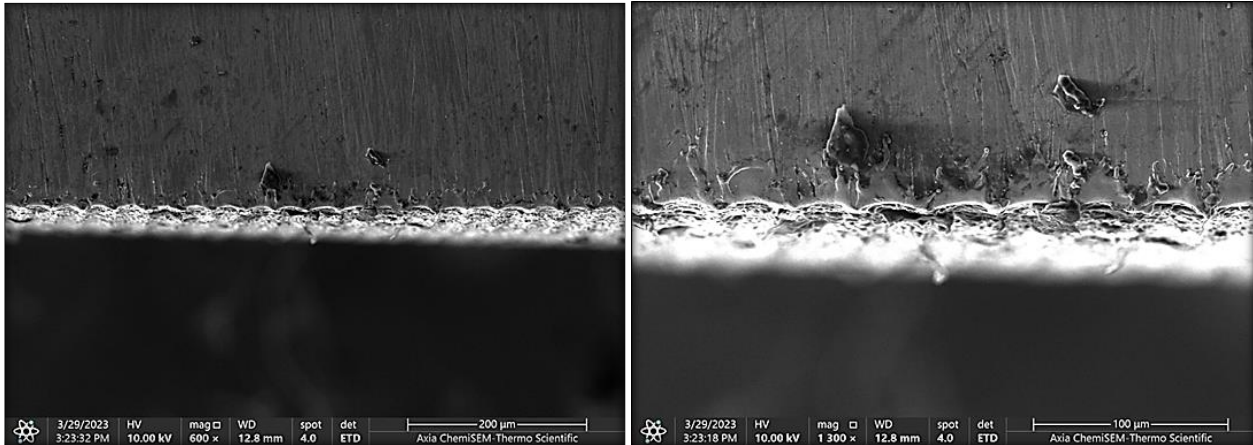
Fig. 6. XRD data of the (a) base metal (before laser treatment) and (b) Sample A3 (after laser treatment).



### 3.4 Effect of Laser Power on the Molten Depth of SS316L

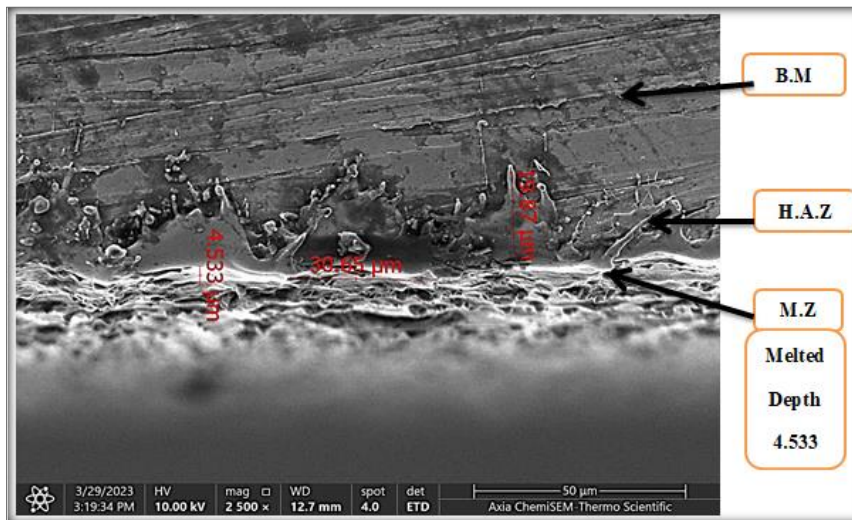
Laser treatment was applied to the outer layer of the sample's surface. SEM examination helped examine the depth of the molten pool. The sample chosen for the SEM test, which was Sample A3 with

a laser power of 7.5 W, depended on the highest reading of the microhardness test. Figure (7c) shows that the melted depth at laser power of 7.5 W was 4.533  $\mu\text{m}$ . Three zones, namely, melted, heat-affected and base metal zones, can be seen in all the figures.



(a)

(b)



(c)

Fig. 7. SEM photo of Sample A3 showing the depth of the molten pool at (a) 600 $\times$ , (b) 1,300 $\times$  and (c) 2,500 $\times$  with laser power of 7.5 W, scanning speed of 3,000 mm/s and frequency of 30 KHz.

## 4. Conclusions

Surface treatments are necessary for materials to achieve desirable mechanical and surface properties. In this study, the surface and mechanical properties of SS316L were enhanced by laser surface treatment. Laser surface treatment generally improved the corrosion resistance, microhardness, wear resistance, fatigue strength and tensile strength

of the materials. The following conclusions were obtained in this study.

1. Surface treatment of SS316L by pulsed fibre laser revealed that the laser affected grain refinement directly.
2. Most samples showed an increase in microhardness. Among the samples, Sample A3 (367.6 HV) with 7.5 W of laser power had the largest increase in microhardness, which was

78.23% more than that of the base metal (206.3 HV).

3. Corrosion resistance at a laser power of 7.5 W increased when the microhardness of the laser-treated materials increased to  $I_{corr.} = 283.51 \text{ nA/cm}^2$  compared with  $I_{corr.} = 18.71 \text{ nA/cm}^2$  of the base metal.
4. In comparison with the base-metal sample, the laser-treated sample showed the presence of the alpha ferrite phase ( $\alpha\text{-Fe}$ ) with an intensified austenite phase ( $\gamma\text{-Fe}$ ) due to grain refinement.
5. According to the SEM data, the depth of the sample treated with laser power of 7.5 W was approximately 4.5  $\mu\text{m}$ .

### Acknowledgement

The authors would like to express their sincere appreciation and gratitude to the University of Baghdad, AL-Khwarizmi College of Engineering, Automated Manufacturing Engineering Department; University of Technology's Production and Metallurgy Department; and University of AL-Nahrain's Laser and Optoelectronic Department for their help in the experimental work.

### References

- [1] B. L. Mordike Surface modification by lasers. In: Materials Science and Technology (Edited by R. W. Cahn, P. Haasen and E. J. Kramer), Vol. 15, pp. 111-136. VCH Verlagsgesellschaft, Weinheim, Germany, 1991.
- [2] Steen W M, Laser material processing, New York: Springer Verlag, 1991.
- [3] Mordike B L, Materials science and technology (eds) RW Cahn, P Haasen, E J Kramer (Weinheim: VCH) 15: 111, 1993.
- [4] Jyoti Menghani, Akash Vyas, Pringal Patel, Harshad Natu, Satish More, "Wear, erosion and corrosion behavior of laser clad high entropy alloy coatings – A review", Volume 38, Part 5, pp. 2824-2829, March 2021.
- [5] Phan Van Truong, Nguyen Van Bo, Nguyen Van Minh, Nguyen Viet Anh, Govindan Suresh Kumar, Mohd. Shkir, "Investigation of corrosion and wear resistance of PEO coated D16T aluminum alloys in the marine tropical climate conditions", Materials Chemistry and Physics Volume 290, 126587, October 2022.
- [6] Sivakumar M, Mudali K U, Raj eswari S, "Investigation of failures in stainless steel orthopedic implant devices; fatigue failure due to improper fixation of a compression bone plate", J. Mater. Sci. 13, pp. 142-145, June 1994.
- [7] Raid Mohammed Hadi, Ziad Aeyad Taha, "Mechanical Properties of AISI 316L Stainless Steel Produced Via Selective Laser Melting", Iraqi Journal of Laser, Volume 21, Issue 1, Pages 51-60, June 2022.
- [8] Ali, Sadaqat, Abdul Rani, Ahmad Majdi, Baig, Zeeshan, Ahmed, Syed Waqar, Hussain, Ghulam, Subramaniam, Krishnan, Hastuty, Sri and Rao, Tadamilla V.V.L.N., "Biocompatibility and corrosion resistance of metallic biomaterials", Corrosion Reviews, vol. 38, no. 5, pp. 381-402, August 2020.
- [9] Yoshimitsu Okazaki, and Emiko G, "Comparison of metal release from various metallic biomaterials in vitro J. of Biomaterials", Biomaterials, (1):11-21, Jan 2005.
- [10] Lubna Abdul Razzaq, Ahmed Qasim Abdullah, "Enhancement of the corrosion resistance of copper metal by laser surface treatment", Iraqi Journal of Physics, Vol.18, No.46, pp. 13-19, September 2020.
- [11] Rahman, A., Salleh, M., Othman, I., Yahaya, S., Al-Zubaidi, S., & Zulkifli, K. "INVESTIGATION OF MECHANICAL & WEAR CHARACTERISTICS OF T6 HEAT TREATED THIXOFORMED ALUMINIUM ALLOY COMPOSITE", Journal of Advanced Manufacturing Technology (JAMT), 14(3), December 2020.
- [12] J.X. Zou, K.M. Zhang, S.Z. Hao, C. Dong, T. Grosdidier, "Mechanisms of hardening, wear and corrosion improvement of 316 L stainless steel by low energy high current pulsed electron beam surface treatment", Thin Solid Films, Volume 519, Issue 4, pp. 1404-1415, 1 December 2010.
- [13] Muna Khethier Abbass, "Effect of Nd-YAG laser treatment on corrosion behavior of AISI316L stainless steel in artificial saliva solution", IOP Conf. Series: Materials Science and Engineering, 518-032006, 2019.
- [14] A.S. Alwan, E.A. Khalid and A.A. Jaddoa, "Effect of Laser Surface Treatment on Corrosion and Wear Characteristics of AISI 304 Stainless Steel", Journal of Mechanical Engineering Research and Developments, Vol. 43, No. 4, pp. 50-59, 2020.
- [15] Swarnima Singh, S. K. Tiwari, Raghuvir Singh, "Influence of laser scanning speed on nitrided Ti6Al4V surface", Surface Engineering 36:12, pp. 1285-1293, October 2020.
- [16] Tangkwampian, R., Srisungsitthisunti, P., Daopiset, S., Kowitwarangkul, P., "Effect of

- Fiber Laser Surface Modification on the Corrosion Behavior of 316L Stainless Steel”, KEM 856, pp. 135–142, August 2020.
- [17] Dongre, Ganesh & Rajurkar, Avadhoot & Gondil, Ramesh & Jaju, Nandan, “Laser surface hardening of SS316L”, IOP Conference Series: Materials Science and Engineering. 1070(1):012107, February 2021.
- [18] Bakhtiari, M., Fayazi Khanigi, A. & Farnia, A., “Improving the Wear Properties of AISI4130 Steel Using Laser Surface Hardening Treatment”, Arab J Sci Eng. September 2023.
- [19] thyssenkrupp Materials (UK) Ltd, Stainless Steel 1.4404 Material Data Sheet, <https://ucpcdn.thyssenkrupp.com/legacy/UCPthyssenkruppBAMXUK/assets.files/material-data-sheets/stainless-steel/stainless-steel-1.4404-316L.pdf> (accessed Nonmember 2017).
- [20] ASM Handbook, volume 9: metallography and microstructures (Edit by George F. Vander Voort), Product code: 06044G ISBN: 978-0-87170-706-2, Page 676, 2004.
- [21] “Hardness - an overview | Science Direct Topics.” <https://www.sciencedirect.com/topics/physics-and-astronomy/hardness> (accessed Mar. 06, 2022).
- [22] Korb L J , Rockwell International and David L Olson 1992 Corrosion Volume 13 of the 9<sup>th</sup> Edition, Metals Handbook, Fourth printing, 1978.
- [23] Sachin Vijay Muley, Amey N. Vidvans, Gajanan P. Chaudhari, Sumit Udainiya, “An assessment of ultra-fine grained 316L stainless steel for implant applications”, Acta Biomaterialia, Volume 30, pp. 408-419, January 2016.
- [24] Ewa Ura-Bińczyk, “Effect of Grain Refinement on the Corrosion Resistance of 316L Stainless Steel”, Materials, 14(24), 7517; December 2021.
- [25] Li, Jianguo; Li, Huan; Liang, Yu; Liu, Pingli; Yang, Lijun; Wang, Yaowei, “Effects of heat input and cooling rate during welding on intergranular corrosion behavior of high nitrogen austenitic stainless steel welded joints”. Corrosion Science, April 2020.

## تقييم تحسين سلوك التآكل والصلابة الدقيقة للفولاذ المقاوم للصدأ 316L باستخدام المعالجة السطحية بليزر الألياف

مصطفى ماجد حسين<sup>1\*</sup> ، ايناس عبد الكريم خالد<sup>2</sup> ، حيدر صغير<sup>3</sup>

<sup>1</sup>قسم هندسة التصنيع المؤتمت، كلية الهندسة الخوارزمي، جامعة بغداد، بغداد، العراق

<sup>3</sup>قسم الهندسة، كلية العلوم والهندسة، جامعة جنوب أركنساس، الولايات المتحدة الأمريكية

\*البريد الإلكتروني: [mostafa.ali2240m@kecbu.uobaghdad.edu.iq](mailto:mostafa.ali2240m@kecbu.uobaghdad.edu.iq)

### المستخلص

تبحث هذه الورقة في كيفية تأثير المعالجة السطحية بليزر الألياف في الصلابة الدقيقة للفولاذ المقاوم للصدأ من النوع 316L ومقاومته للتآكل. معلمات الليزر المستخدمة في هذا الفحص هي طاقة الليزر بأربع قراءات مختلفة و بتردد مسح ثابت و سرعة ثابتة مطبقة على عينات الفولاذ المقاوم للصدأ 316L. وتم استخدام جهاز اختبار صلابة فيكرز الرقمي الصغير لقياس الصلابة الدقيقة للعينات بوحدة HV قبل وبعد العلاج بالليزر. وتم استخدام تقنية الاستقطاب الديناميكي الدوري TAFEL لدراسة سلوك التآكل. و تحت دراسة البنية المجهرية للمعدن الأساسي وتأثير قوة الليزر باستخدام المجهر الضوئي (OM). وتم تحديد المراحل قبل وبعد العلاج بالليزر باستخدام حيود الأشعة السينية XRD. تم فحص المقطع العرضي للمناطق المتأثرة بالحرارة وعمق البركة المنصهرة باستخدام المجهر الإلكتروني الماسح (SEM). وقد كشفت النتائج أن العلاج بالليزر أثر في تغييرات المرحلة الانتقالية المجهرية. فضلا عن ذلك، تحسنت الصلابة الدقيقة إلى 78.23% مع زيادة طاقة الليزر؛ بالاعتماد على المعلمات المطبقة مقارنة بمتوسط الصلابة الدقيقة للمعدن الأساسي. أدت زيادة الصلابة الدقيقة إلى تعزيز مقاومة التآكل بشكل كبير إلى 36.13% مقارنة بالمعدن الأساسي.